

Supporting Information

Mechanistic studies on the nitrite-catalyzed reductive nitrosylation of highly charged anionic and cationic Fe^{III}-porphyrin complexes

Joo-Eun Jee and Rudi van Eldik

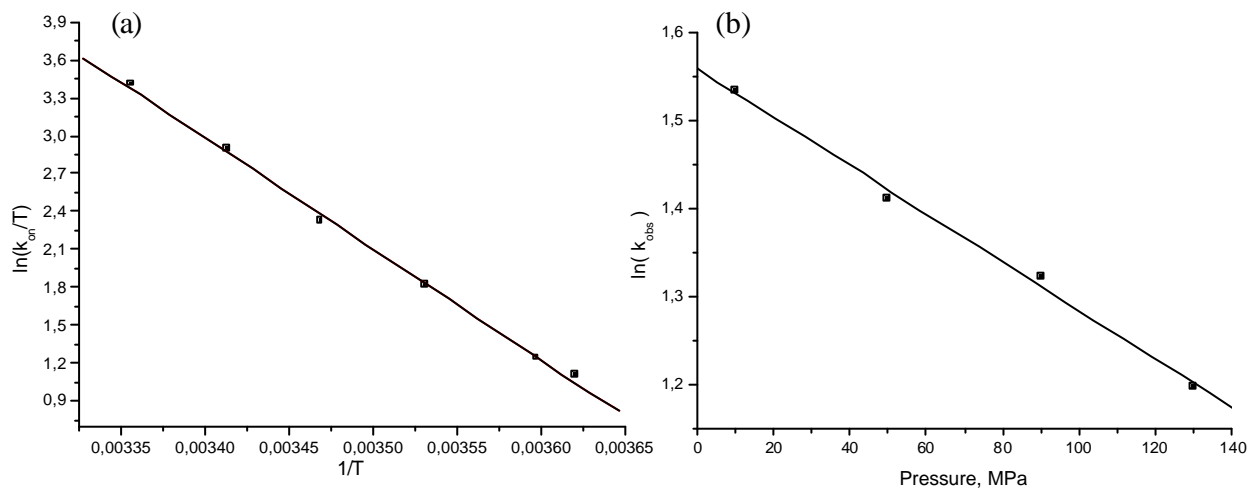


Figure S1. (a) Plot of $\ln(k_{\text{obs}}/T)$ versus $1/T$ in the temperature range 5 – 25 °C for the binding of nitrite to $(P^{8+})Fe^{III}(H_2O)_2$. Experimental conditions: $[(P^{8+})Fe^{III}]^{9+} = 7.5 \times 10^{-6}$ M, $\lambda_{\text{det}} = 430$ nm, $I = 0.1$ M (with KNO_3), pH 2.0 (b) Plot of $\ln(k_{\text{obs}})$ versus pressure for the reaction of $(P^{8+})Fe^{III}(H_2O)_2$ with NO_2^- in the pressure range 10 – 130 MPa. Experimental conditions as in (a), $[NO_2^-] = 6$ mM, $\lambda_{\text{det}} = 430$ nm, temp = 2.5 °C.

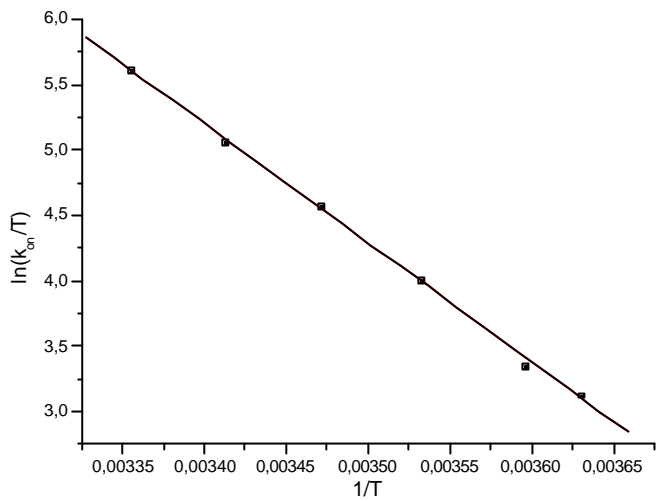


Figure S2. Plot of $\ln(k_{\text{obs}}/T)$ versus $1/T$ for nitrite binding to $(\text{P}^{8+})\text{Fe}^{\text{III}}(\text{H}_2\text{O})_2$. Experimental conditions: $[(\text{P}^{8+})\text{Fe}^{\text{III}}]^{9+} = 7.5 \times 10^{-6}$ M, $[\text{NO}_2^-] = 1$ mM, $\lambda_{\text{det}} = 430$ nm, temp = 25 °C, $I = 0.1$ M (with KNO_3), pH 4.0

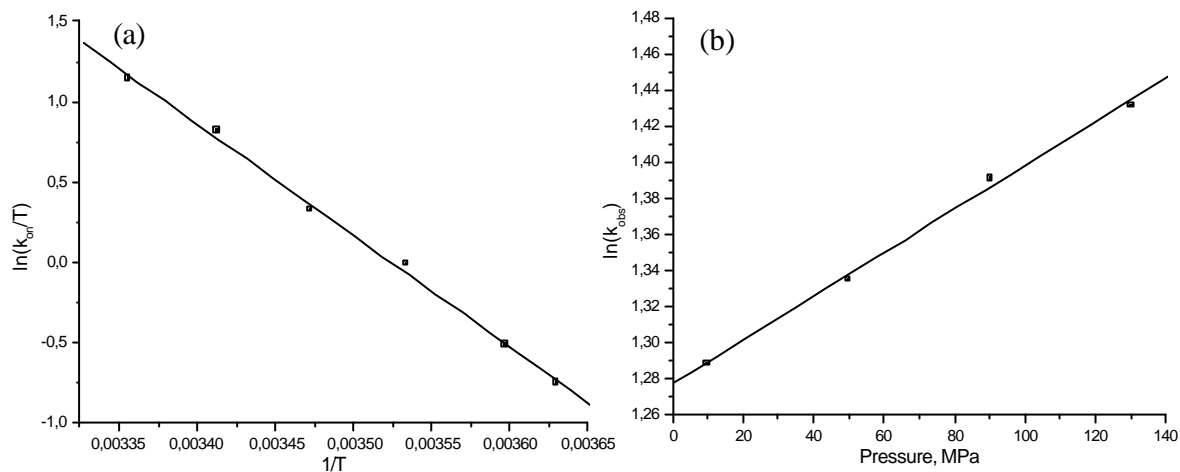


Figure S3. (a) Plot of $\ln(k_{\text{obs}}/T)$ versus $1/T$ in the temperature range 5 – 25 °C for the binding of NO_2^- to $(\text{P}^{8+})\text{Fe}^{\text{III}}(\text{OH})$. Experimental conditions: $[(\text{P}^{8+})\text{Fe}^{\text{III}}]^{9+} = 8.5 \times 10^{-6}$ M, $[\text{NO}_2^-] = 25$ mM, $\lambda_{\text{det}} = 435$ nm, $I = 0.1$ M (with KNO_3), pH 8.0. (b) Plot of $\ln(k_{\text{obs}})$ versus pressure for the reaction of $(\text{P}^{8+})\text{Fe}^{\text{III}}(\text{OH})$ with NO_2^- in the pressure range 10 – 130 MPa. Experimental conditions as in (a), $[\text{NO}_2^-] = 10$ mM.

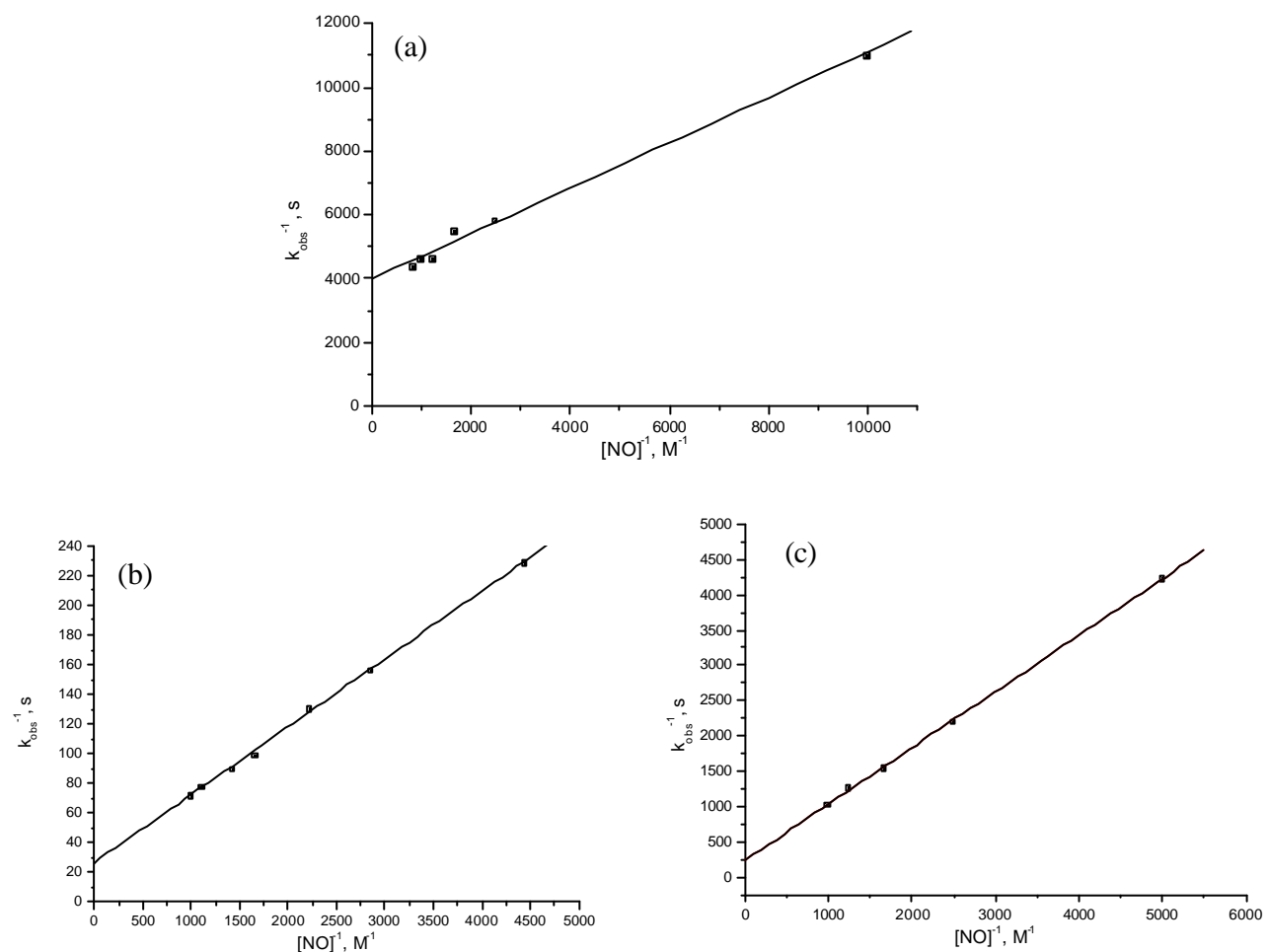


Figure S4. (a) Plot of $(k_{\text{obs}})^{-1}$ vs. $[\text{NO}]^{-1}$ for reductive nitrosylation of $(\text{P}^{8-})\text{Fe}^{\text{II}}(\text{OH}_2)(\text{NO}^+)$ at pH 7, (b) $(\text{P}^{8+})\text{Fe}^{\text{II}}(\text{OH}_2)(\text{NO}^+)$ at pH 2 and (c) $(\text{P}^{8+})\text{Fe}^{\text{II}}(\text{OH})(\text{NO}^+)$ at pH 8. These plots are based on the kinetic data reported in Figures 7, 9 and 11. For experimental conditions see the mentioned figures.

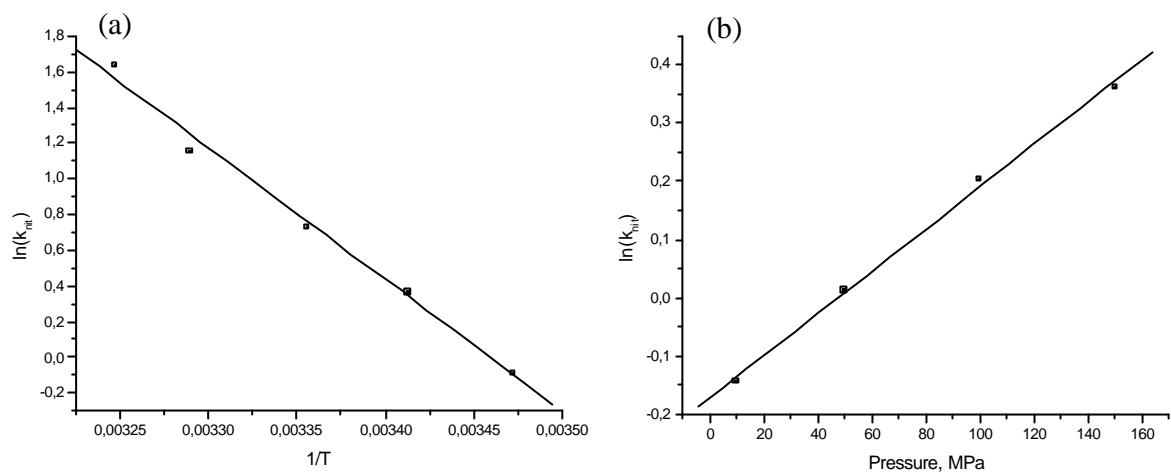


Figure S5. (a) Temperature dependence of reductive nitrosylation of $(P^{8-})Fe^{II}(H_2O)(NO^+)$ by NO/nitrite. (b) Pressure dependence. Experimental conditions: (a) $[Fe^{III}(P^{8-})]^{7-} = 2.0 \times 10^{-5}$ M, $[NO] = 1$ mM, $[NO_2^-] = 1.5$ mM, $I = 0.1$ M (with $NaClO_4$), pH 7.0 with Bis-tris buffer; (b) $[NO_2^-] = 0.5$ mM, temp = 13.5 °C, $\lambda_{\text{det}} = 426$ nm.

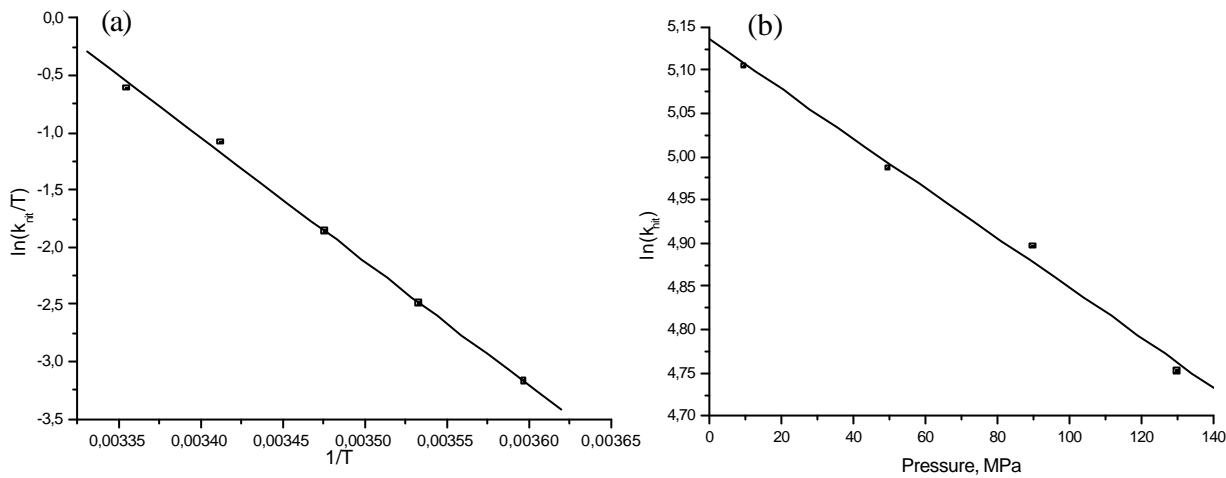


Figure S6. (a) Plot of $\ln(k_{\text{nit}}/T)$ versus $1/T$ for reductive nitrosylation of $(\text{P}^{8+})\text{Fe}^{\text{II}}(\text{H}_2\text{O})(\text{NO}^+)$ by NO/nitrite (where $k_{\text{nit}} = k_{\text{obs}}(1 + K_{\text{NO}})/K_{\text{NO}}[\text{NO}]$ at constant $[\text{NO}_2^-]$) in the temperature range 5 – 25 °C, $[\text{NO}_2^-] = 1 \text{ mM}$, $\lambda_{\text{det}} = 431 \text{ nm}$. (b) Pressure dependence, Experimental conditions: $(\text{P}^{8+})\text{Fe}^{\text{III}}{}^{9+} = 1.0 \times 10^{-5} \text{ M}$, $[\text{NO}] = 1 \text{ mM}$, $[\text{NO}_2^-] = 1 \text{ mM}$, temp = 25.0 °C, $\lambda_{\text{det}} = 431 \text{ nm}$, $I = 0.1 \text{ M} (\text{KNO}_3)$, pH 2.0

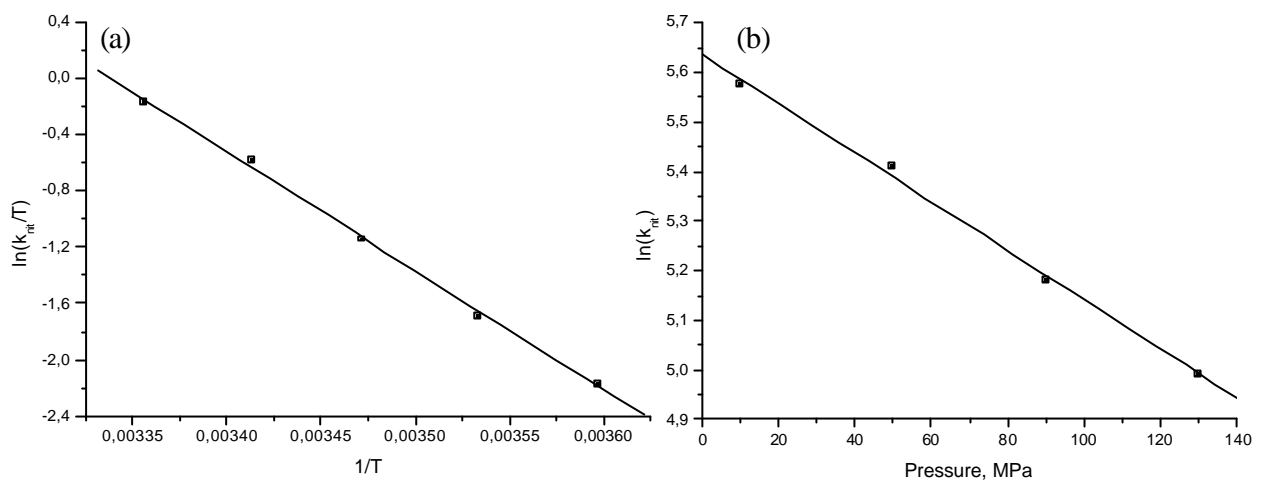


Figure S7. (a) Plot of $\ln(k_{\text{nit}}/T)$ versus $1/T$ for reductive nitrosylation of $(\text{P}^{8+})\text{Fe}^{\text{II}}(\text{H}_2\text{O})(\text{NO}^+)$ by NO/nitrite in the temperature range 5 – 25 °C, $[\text{NO}_2^-] = 1 \text{ mM}$, $\lambda_{\text{det}} = 431 \text{ nm}$. (b) Pressure dependence, Experimental conditions: $[(\text{P}^{8+})\text{Fe}^{\text{III}}]^{9+} = 1.0 \times 10^{-5} \text{ M}$, $[\text{NO}] = 1 \text{ mM}$, $[\text{NO}_2^-] = 0.1 \text{ mM}$, $\lambda_{\text{det}} = 431 \text{ nm}$, $I = 0.1 \text{ M}$, pH 4.0

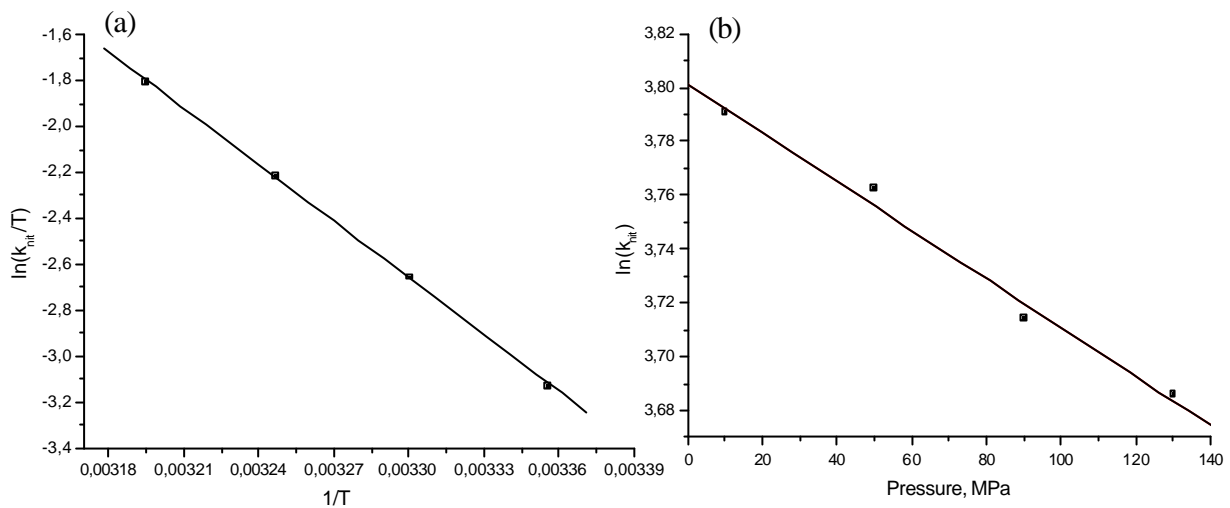


Figure S8. (a) Plot of $\ln(k_{\text{nit}}/T)$ versus $1/T$ in the temperature range 25 – 40 °C for reductive nitrosylation of $(\text{P}^{8+})\text{Fe}^{\text{II}}(\text{OH})(\text{NO}^+)$ by NO/nitrite. (b) Plot of $\ln(k_{\text{nit}})$ versus pressure in the range 10 – 130 MPa, $[\text{NO}] = 0.5 \text{ mM}$, $[\text{NO}_2^-] = 0.5 \text{ mM}$. Experimental conditions: $[(\text{P}^{8+})\text{Fe}^{\text{III}}] = 8.5 \times 10^{-6} \text{ M}$, temp = 25 °C, $\lambda_{\text{det}} = 435 \text{ nm}$, $I = 0.1 \text{ M}$ (with KNO_3), pH 8.0

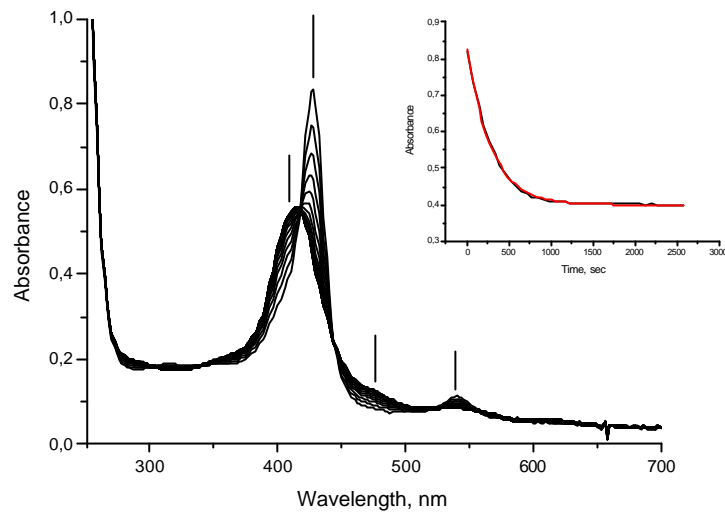


Figure S9. Spectral changes observed following the binding of NO to $(P^{8-})Fe^{III}(H_2O)_2$. Inset: kinetic trace of absorbance at 426 nm vs. time fitted to a single exponential function. Experimental conditions: $[(P^{8-})Fe^{III}]^{7-} = 1 \times 10^{-5}$ M, [NO] = 1 mM, [added NO_2^-] = 2 mM, temp = 25.0 °C, I = 0.1 M (with NaClO₄) pH = 7.0. The observed rate constant is $k_{obs} = 3.54 \times 10^{-3}$ s⁻¹.

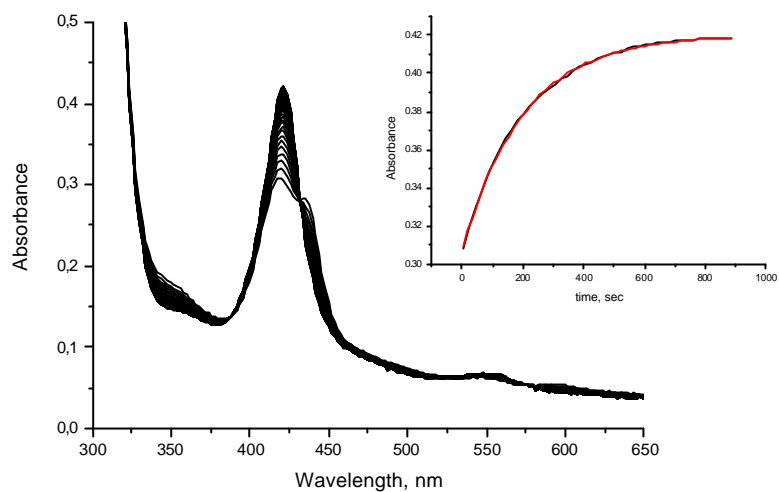


Figure S10. Spectral changes observed for the reaction of $(P^{8+})Fe^{II}(OH)(NO^+)$ with NO/nitrite. Inset: kinetic trace of absorbance vs. time at 422 nm fitted with a single exponential function. Experimental conditions: $[(P^{8+})Fe^{III}]^{9+} = 7.5 \times 10^{-6}$ M, $[NO] = 1$ mM, $[NO_2^-] = 2$ mM, temp = 25.0 °C, pH 8.0, $I = 0.1$ M (KNO_3). The spectra were recorded every 20 sec.